Elastic Stability of Biaxially Loaded Longitudinally Stiffened Composite Structures

A. V. VISWANATHAN* AND M. TAMEKUNI†
The Boeing Commercial Airplane Company, Seattle, Wash.
AND
LEONARD L. TRIPP‡
The Boeing Computer Services, Seattle, Wash.

A linear analysis method is presented for the elastic stability of structures of uniform cross section, that may be idealized as an assemblage of laminated plate-strips, flat and curved, and beams. Each plate-strip and beam covers the entire length of the structure and is simply supported on the edges normal to the longitudinal axis. Arbitrary boundary conditions may be specified on any external longitudinal side of plate-strips. The structure or selected plate-strips may be loaded in any desired combination of in-plane biaxial loads. The analysis simultaneously considers all modes of instability and is applicable for the buckling of laminated composite structures. Some numerical results are presented to indicate possible applications. Predicting a previously unknown buckling mode shape for a zee-stiffened panel demonstrates the generality of this method. The results for some conceptually advanced structural panels illustrate some applications of the curved plate-strips. Results also confirm the experimentally observed superiority of bonded over riveted connections and show, for the example considered, the significance of ignoring offsets effects in stability analysis.

Nomenclature§

a	= length of the structure
A_{ij}, B_{ij}, D_{ij} $(i,j = 1,2,6)$	= elements of the extensional, coupling and bending stiffness matrices, respectively
b	= developed width of plate-strip
I_p	= beam polar moment of inertia
I_{yy}, I_{zz}	= beam moments of inertia
J	= beam torsion constant
m	= number of axial half-waves
M_{11}, M_{12}, M_{22}	= moment resultants
M_x	= torque on beam element
N_{11}, N_{12}, N_{22}	= stress resultants
$\bar{N}_{11}, \bar{N}_{22}$	= applied in-plane loads on plate-strips
P	= axial load in beams induced by buckling
$\bar{P}_b$	= applied axial load on beams
q_y, q_z	= lateral shears on beam
R	= midplane radius of curved plate-strip
u, v, w	= buckling displacements
Γ	= beam warping constant

Introduction

CRITICAL regions of structures utilizing thin plate construction are prone to buckling. In aerospace structures the application of new design concepts[1] and new materials such as fiber reinforced laminated composites[2] have precipitated the need for corresponding improvements in analysis techniques. Attention is confined here to structural components that may, in general, be idealized as an assemblage of a series of laminated plate-strips (flat and curved) and laminated beam elements interlinked along their longitudinal edges. The individual plate-strips and beams extend over the full length of the component and are of uniform cross section. The edges of each plate-strip normal to the longitudinal axis and the ends of the beams are assumed to be simply supported with no restrictions on the axial (warping) displacements. Longitudinally stiffened panels such as those in Fig. 1 are typical examples. The figure also shows examples of beam elements.

A unified linear stability analysis limited to structural com-

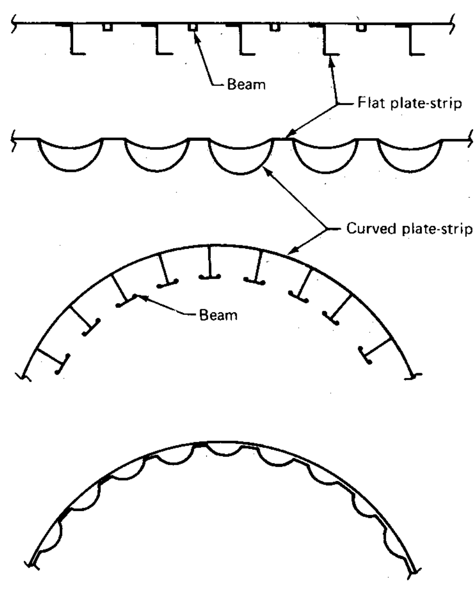

Fig. 1 Cross section of typical stiffened panels.

Presented as Paper 73-367 at the AIAA/ASME/SAE 14th Structures, Structural Dynamics, and Materials Conference, Williamsburg, Va., March 20–22, 1973; submitted April 9, 1973; revision received June 6, 1973. The authors are thankful to C. R. Gagnon and P. Lu of the Boeing Computer Services for significant numerical analysis support. Particular appreciation is expressed to M. F. Card and M. Stein of NASA Langley Research Center and R. E. Miller Jr., of the Boeing Commercial Airplane Company, for interesting discussions and suggestions. The work was performed as part of NASA Contract NAS1-8858.

Index categories: Structural Stability Analysis; Structural Composite Materials (Including Coatings).

* Member AIAA.

† Technical Staff, Stress Analysis Research.

‡ Scientific Computing Staff, Structures Systems.

§ A subscript preceded by a comma indicates partial differentiation with respect to the subscript.

ponents idealized from flat plate-strip and beams and subjected to axial compression is given in Ref. 3. The basic equations used therein do not correctly account for the possibility of predominantly in-plane buckling displacements in the individual plate strips. This becomes evident when considering the Euler type buckling of a square tube. Two of the plate-strips (forming two opposite sides of the tube) have only out-of-plane displacements, whereas the other two have only in-plane displacements. Thus, the analysis of Ref. 3 would yield erroneous buckling load; in fact, twice the exact value. Further, the formulation used results in an unsymmetric "buckling determinant," necessitating the use of repetitive determinant evaluations to calculate the buckling load. The disadvantages of this method, as discussed in Ref. 4, are the need to use small load increments resulting in uneconomical computation time and the possibility of missing the lowest buckling load.

The present analysis, in addition to overcoming the above deficiencies, also includes the use of laminated curved plate-strips to idealize the structural component. They have constant curvature with zero gaussian curvature and are, in general, laminated. Equations derived using variational principles and based on the geometry of shell deformations given in Ref. 5, are used for these plate-strips.

Elementary theory of bending and torsion is used for the beam elements. The external loading on them is uniform and axial. The physical properties of laminated beams are calculated in an approximate manner.

Symmetric stiffness matrices are derived relating the buckling displacements and the corresponding forces along the sides of the individual plate-strips and along the axis of individual beams making up the structural components. The over-all stiffness matrix (symmetric) of the component, which is obtained by suitably merging the individual stiffness matrices, corresponds to the unsymmetric buckling determinant of Ref. 3, and is considerably smaller in size. The symmetry, enables the use of the algorithm described in Ref. 6, to isolate with certainty and in relatively fewer load iterations, the lowest buckling load. A primary requirement of this algorithm is an upper bound for the buckling load, resulting from completely restraining all the interlinked junction lines of plate-strips and beams. Such a bounding value is readily obtained by applying the Galerkin method[7] for each plate-strip.

The elements of the stiffness matrix are transcendental functions of the external loadings and the half-wave length of buckling. For each assumed half-wave length (or integer number of longitudinal half-waves), the lowest level of applied loads at which the determinant of the over-all stiffness matrix vanishes is a buckling load. The lowest of these loads is then the critical load. It is stressed that no prior assumption of the buckling mode is made, except that the axial half-wavelength of buckling is the same in all plate-strips and beam elements. The buckling mode shape is obtained from the eigenvector solution of the stiffness matrix at the critical load. The usefulness of the buckling mode shape plots in achieving efficient design of stiffened plates is discussed and illustrated in Refs. 3 and 8.

The analysis considers offsets between elements and effects of arbitrary elastic restraints along any external longitudinal side (i.e., not connected to other elements) of the flat or curved plate-strip elements. The basic assumptions governing the analysis are as follows. a) The material is linearly elastic. b) Each lamina is orthotropic. c) The Kirchhoff-Love hypothesis is used for each plate-strip and beam. d) Effects of prebuckling deformations are ignored. Thus, at buckling each plate-strip, whether flat or curved, is, in general, in a state of uniform biaxial inplane loading. Each beam is under uniform axial load. e) The edges of each plate-strip normal to the longitudinal axis are simply supported in the classical sense. So are the ends of the beams. A computer program "BUCLASP2" based on the present analysis has been written for the CDC 6600 computer.[9]

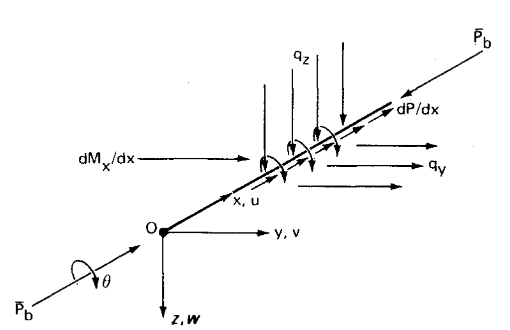

Fig. 2 Displacements and forces in beams due to buckling.

Basic Equations

Laminated Curved and Flat Plate-Strips

The equations given below for the curved plate-strips degenerate to those of flat plate-strips when the radius $R \to \infty$. The midplane of the laminate is chosen as the reference plane. The strains and curvature changes in this plane, in terms of its displacements u, v and w are[5]

$$\begin{aligned} \varepsilon_x^{\,0} &= u,_x; & \kappa_x^{\,0} &= -w,_{xx} \\ \varepsilon_y^{\,0} &= v,_y - w/R; & \kappa_y^{\,0} &= -w,_{yy} - (1/R)v,_y \\ \varepsilon_{xy}^{\,0} &= u,_y + v,_x; & \kappa_{xy}^{\,0} &= -2w,_{xy} - (2/R)v,_x \end{aligned} \tag{1}$$

The stress and moment resultants in the reference plane are[10]

$$\begin{Bmatrix} N_{11} \\ N_{22} \\ N_{12} \\ M_{11} \\ M_{22} \\ M_{12} \end{Bmatrix} = \begin{bmatrix} A_{11} & A_{12} & 0 & B_{11} & B_{12} & 0 \\ & A_{22} & 0 & B_{12} & B_{22} & 0 \\ & & A_{66} & 0 & 0 & B_{66} \\ & & & D_{11} & D_{12} & 0 \\ \text{SYM.} & & & & D_{22} & 0 \\ & & & & & D_{66} \end{bmatrix} \begin{Bmatrix} \varepsilon_x^{\,0} \\ \varepsilon_y \\ \varepsilon_{xy}^{\,0} \\ \kappa_x^{\,0} \\ \kappa_y^{\,0} \\ \kappa_{xy}^{\,0} \end{Bmatrix} \tag{2}$$

When the orthotropic axes for each lamina do not coincide with the laminate axes, the "16" and "26" subscripted elements are nonzero. In practical structures these elements are of relatively small magnitude and may be ignored. This simplification, while considerably reducing the complexity of the analysis, is, however, not thought to be unduly restrictive.

Using variational principles in the manner of Refs. 11 and 12, and ignoring prebuckling deformations, the "stability equations" of the curved plate-strip subjected to biaxial in-plane loads $\bar{N}_{11}$ and $\bar{N}_{22}$ (per unit length) are derived as

$$N_{11,x} + N_{12,y} - \bar{N}_{11}u,_{xx} - \bar{N}_{22}u,_{yy} = 0 \tag{3}$$

$$N_{22,y} + N_{12,x} - (1/R)(M_{22,y} + 2M_{12,x}) - \bar{N}_{11}v,_{xx} - \bar{N}_{22}[v,_{yy} - (2/R)w,_y - (1/R^2)v] = 0 \tag{4}$$

$$M_{11,xx} + M_{22,yy} + 2M_{12,xy} + (1/R)N_{22} - \bar{N}_{11}w,_{xx} - \bar{N}_{22}[(2/R)v,_y + w,_{yy} - (1/R^2)w] = 0 \tag{5}$$

The consistent boundary conditions are, along any side $y = \text{const}$

$$w = 0 \text{ or } M_{22,y} + 2M_{12,x} - \bar{N}_{22}[(v/R) + w,_y] = 0 \tag{6}$$

$$[w,_y + (v/R)] = 0 \text{ or } M_{22} = 0 \tag{7}$$

$$v = 0 \text{ or } N_{22} - \bar{N}_{22}[v,_y - (w/R)] = 0 \tag{8}$$

$$u = 0 \text{ or } N_{12} - \bar{N}_{22}u,_y = 0 \tag{9}$$

Similarly along any edge $x = \text{const}$

$$w = 0 \text{ or } M_{11,x} + 2M_{12,y} - \bar{N}_{11}w,_x = 0 \tag{10}$$

$$w,_x = 0 \text{ or } M_{11} = 0 \tag{11}$$

$$v = 0 \text{ or } N_{12} - \bar{N}_{11}v,_x = 0 \tag{12}$$

$$u = 0 \text{ or } N_{11} - \bar{N}_{11}u,_x = 0 \tag{13}$$

Laminated Beams

The theory of torsion and flexture[13] gives the following equations for a beam subjected to axial compressive force $\bar{P}_b$:

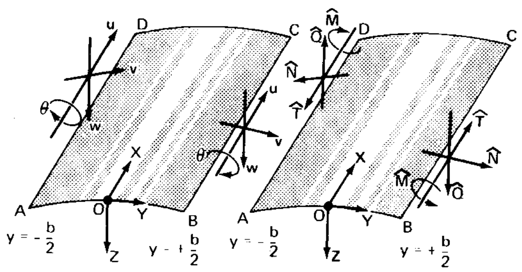

Fig. 3 Displacements and forces due to buckling sides of a plate-strip.

$$q_z = E_{11}I_{yy}\,d^4w/dx^4 + \bar{P}_b\,d^2w/dx^2 + \bar{P}_b\,y_m\,d^2\theta/(dx^2) \tag{14}$$

$$dM_x/dx = E_{11}\Gamma\,d^4\theta/dx^4 + (\bar{\sigma}I_p - G_{23}J)\,d^2\theta/dx^2 + \bar{P}_b\,y_m\,d^2w/dx^2 - \bar{P}_b\,z_m\,d^2v/dx^2 \tag{15}$$

$$q_y = E_{11}I_{zz}\,d^4v/dx^4 + \bar{P}_b\,d^2v/dx^2 - \bar{P}_b\,z_m\,d^2\theta/dx^2 \tag{16}$$

$$dP/dx = -E_{11}A_b\,d^2u/dx^2 \tag{17}$$

y_m and z_m are the distances measured parallel to the principal axes y and z, respectively, from the shear center to the neutral axis of the beam. Figure 2 shows the beam displacements and the forces defined in Eqs. (14–17). Approximate methods to evaluate the various gross beam properties involved for the more common types of beams, namely, laminated circular beams and laminated rectangular beams are given in Ref. 14.

Stability Analysis

Stiffness of Curved and Flat Plate-Strips

Stiffnesses relating the buckling displacements and the corresponding forces along the sides $y = \pm b/2$ of the plate-strips (see Fig. 3) are required for the stability analysis. The displacements involved are

$$w, (\theta = w_{,y} + v/R), \quad v \text{ and } u \tag{18}$$

The corresponding forces are

$$\hat{Q} = Q_2 - \bar{N}_{22}(w_{,y} + v/R)(\text{where } Q_2 = M_{22,y} + 2M_{12,x})$$

$$\hat{M} = M_{22}$$

$$\hat{N} = N_{22} - \bar{N}_{22}(v_{,y} - w/R) \tag{19}$$

and

$$\hat{T} = N_{12} - \bar{N}_{22}u_{,y}$$

The buckling displacement functions are chosen as

$$w = \sum_{i=1}^{8} W_i e^{\beta_i} \sin\alpha \qquad \alpha = m\pi x/a$$

$$v = \sum_{i=1}^{8} V_i e^{\beta_i} \sin\alpha \qquad \beta_i = p_i \pi y/a \tag{20}$$

$$u = \sum_{i=1}^{8} U_i e^{\beta_i} \cos\alpha$$

p_i are the roots of the characteristics equation discussed later. The preceding functions are chosen to satisfy ab initio the simply supported boundary conditions defined by

$$w = M_{11} = v = (N_{11} - \bar{N}_{11}u_{,x}) = 0 \tag{21}$$

along the edges $x = 0$ and $x = a$. At any particular level of external loads $\bar{N}_{11}$ and $\bar{N}_{22}$, on substituting a typical term from Eqs. (20) and Eqs. (1) and (2) into Eqs. (3–5), yields

$$\begin{bmatrix} R_{11} & R_{12} & R_{13} \\ R_{21} & R_{22} & R_{23} \\ R_{31} & R_{32} & R_{33} \end{bmatrix} \begin{Bmatrix} U_i \\ V_i \\ W_i \end{Bmatrix} = 0 \tag{22}$$

A characteristic polynomial in the form

$$K_8 p_i^8 + K_6 p_i^6 + K_4 p_i^4 + K_2 p_i^2 + K_0 = 0 \tag{23}$$

resulting from the determinant of the matrix $[R]$ yields eight values of p_i, which are real or complex conjugates. Also, from the first two of Eqs. (22), U_i and V_i may be expressed in terms of W_i. Superscripts $-$ and $+$ are used hereafter to denote the two sides $y = -b/2$ and $y = +b/2$, respectively, of the plate-strip. Using these values of y in Eqs. (20) the displacements specified by Eqs. (18) are written as

$$\begin{Bmatrix} d^- \\ d^+ \end{Bmatrix} = \begin{bmatrix} c_1 & 0 \\ 0 & c_1 \end{bmatrix} [X_1]\{W_i\} \tag{24}$$

where

$$d = \{w, \theta, v, u\}^T$$

$$c_1 = \ulcorner \sin\alpha, \sin\alpha, \sin\alpha, \cos\alpha \lrcorner$$

$$W_i = \{W_1 \ldots W_8\}^T$$

and X_1 is an 8×8 matrix.

Similarly the forces specified by Eq. (19) are given by

$$\begin{Bmatrix} f^- \\ f^+ \end{Bmatrix} = \begin{bmatrix} c_1 & 0 \\ 0 & c_1 \end{bmatrix} [X_2]\{W_i\} \tag{25}$$

where

$$f = \{\hat{Q}, \hat{M}, \hat{N}, \hat{T}\}^T$$

and X_2 is an 8×8 matrix.

Since the number of axial half-waves of buckling, m, is identical in all plate-strips and beams making up the structure, c_1 matrix can be separated out and readily dropped from further consideration.

Substituting for W_i from Eq. (24) into Eq. (25), the stiffness matrix $[s]$ of the plate-strip is obtained as

$$\begin{Bmatrix} f^- \\ f^+ \end{Bmatrix} = [s] \begin{Bmatrix} d^- \\ d^+ \end{Bmatrix} \tag{26}$$

where

$$s = \begin{bmatrix} s_{11} & s_{12} \\ s_{21} & s_{22} \end{bmatrix} = X_2(X_1)^{-1} \tag{27}$$

The symmetric matrix $[s]$ is 8×8 and is with respect to the local coordinate system. The elements of this matrix are transcendental functions of the half-wavelength of buckling (a/m) and the applied loads $\bar{N}_{11}$ and $\bar{N}_{22}$.

In the structures for which the present stability analysis is applicable, some plate-strips may have specified boundary conditions along an external longitudinal (x) side, not connected to other plate-strips or beams. Such conditions may be defined by a diagonal matrix

$$k_0 = \ulcorner k_w, k_\theta, k_v, k_u \lrcorner \tag{28}$$

formed from the spring constants in the directions of the subscripted displacements.

Consider the side $y = +b/2$ of the plate-strip being elastically restrained by spring stiffness of Eq. (28). Then

$$f^+ = -k_0{}^+ d^+ \tag{29}$$

Also from Eq. (26)

$$f^+ = s_{21}d^- + s_{22}d^+ \tag{30}$$

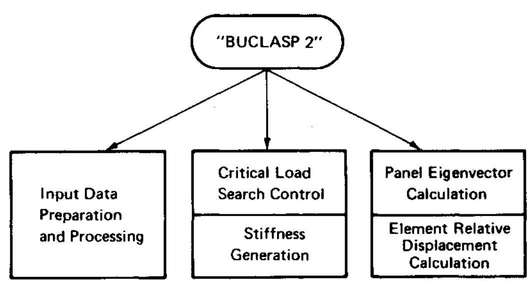

Fig. 4 Basic layout of the computer program.

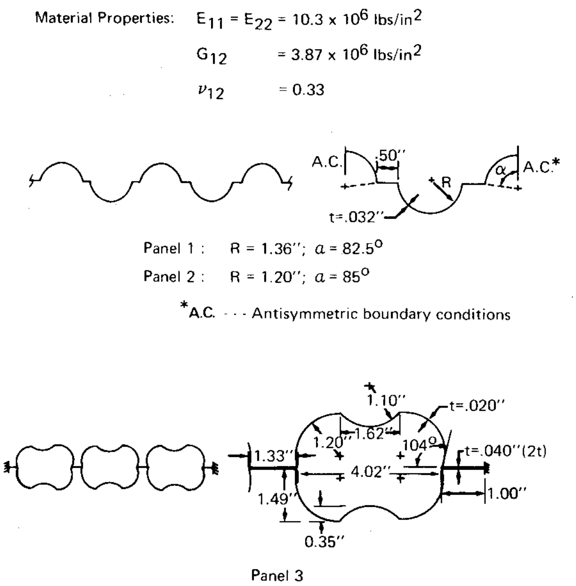

Fig. 5 Conceptually advanced structural panels.

Using Eqs. (29) and (30) in the expression for f^- from Eq. (26) results in

$$f^- = s_k^- d^- \tag{31}$$

where s_k^- is the reduced stiffness matrix (4×4) for the plate-strip when the side $y = +b/2$ is elastically restrained and is with respect to the local coordinate system. A similar equation may be written when the side $y = -b/2$ is elastically restrained.

In idealizing a structure of uniform cross section as an assembly of plate-strips (flat and curved) and beams, possible offsets necessitate an appropriate offset transformation. Also, the intersecting angles between various plate-strips and beams being arbitrary, it is convenient to transform the stiffnesses to common global axes. Such procedures are discussed in detail in Ref. 14.

Stiffness of Beam Elements

The assumed buckling displacement functions satisfying the simply supported conditions at $x = 0$ and $x = a$ are

$$\begin{aligned} w &= W_b \sin\alpha \\ \theta &= \Theta_b \sin\alpha \\ v &= V_b \sin\alpha \\ u &= U_b \cos\alpha \end{aligned} \tag{32}$$

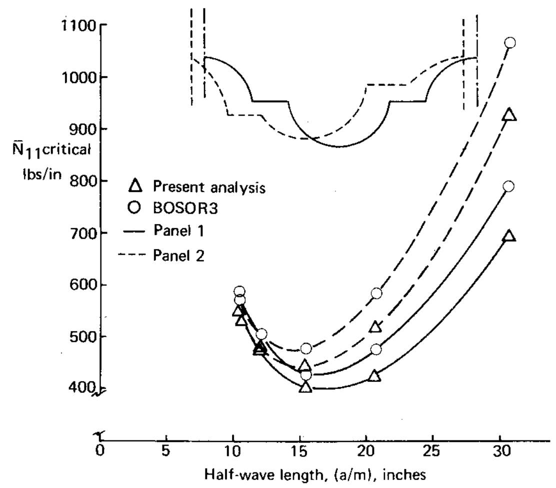

Fig. 6 Buckling results for panels 1 and 2.

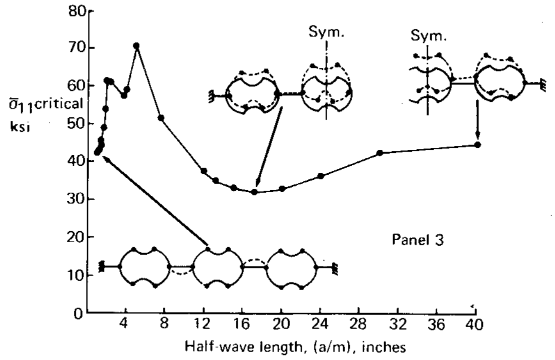

Fig. 7 Buckling results for panel 3.

On substituting these displacements in Eqs. (14–17) and again dropping the axial variations as for the plate-strips, the stiffness matrix of the beam element is readily obtained as

$$f_b = s_b d_b \tag{33}$$

where

$$f_b = \{q_z, dM_x/dx, q_y, dP/dx\}^T$$
$$d_b = \{w, \theta, v, u\}^T$$

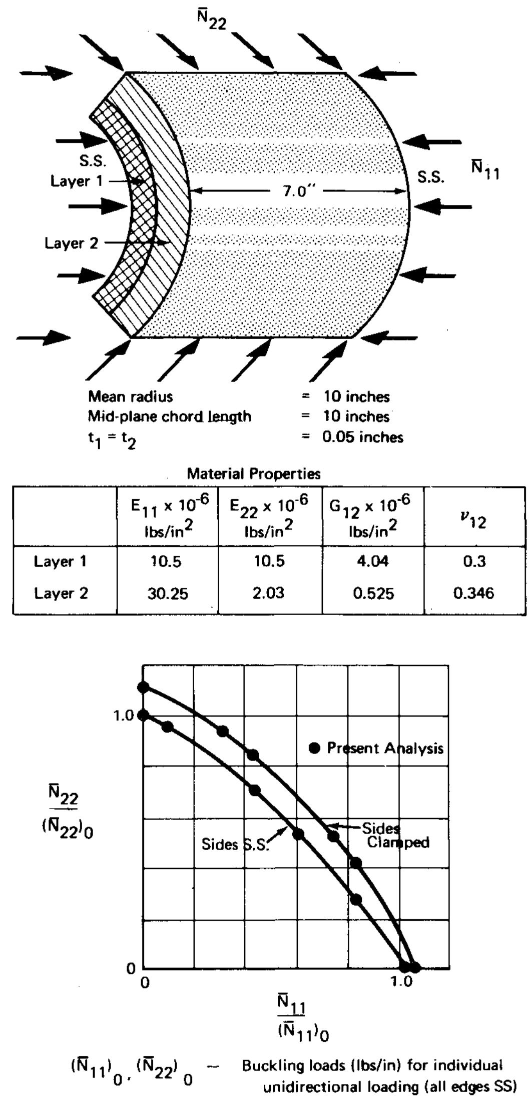

	$E_{11} \times 10^{-6}$ lbs/in^2	$E_{22} \times 10^{-6}$ lbs/in^2	$G_{12} \times 10^{-6}$ lbs/in^2	ν_{12}
Layer 1	10.5	10.5	4.04	0.3
Layer 2	30.25	2.03	0.525	0.346

Fig. 8 Buckling of a biaxially loaded curved plate.

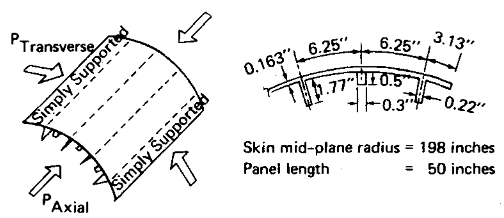

Material Data

Element	$E_{11} \times 10^{-6}$ lbs/in^2	$E_{22} \times 10^{-6}$ lbs/in^2	$G_{12} \times 10^{-6}$ lbs/in^2	$G_{23} \times 10^{-6}$ lbs/in^2	ν_{12}
Plate	10.5	10.5	3.975	---	0.32
Beam	30.0	---	---	0.8	---

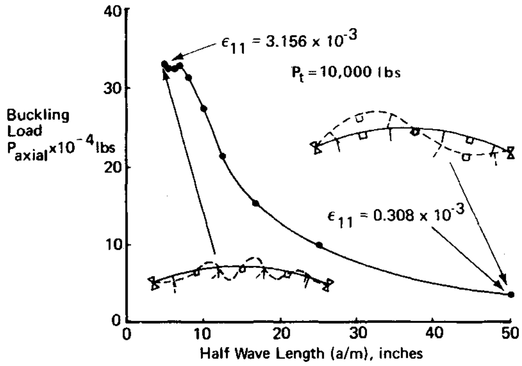

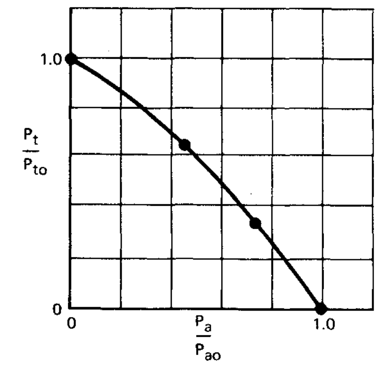

Curved Panel

P_{ao}, P_{to} – Buckling loads (lbs) for individual unidirectional loading in the axial and transverse directions, respectively

Fig. 9 Buckling of a biaxially loaded curved stiffened panel.

and s_b is the 4×4 stiffness matrix with respect to the local axes. This may be transformed to the global axes system as for the plate-strips.

Stability Formulation

The structure is first idealized as an assemblage of suitable plate-strips (flat and curved) and beams. This procedure identifies any offsets present. It is possible to differentiate between bonded and riveted connections as discussed in Ref. 9. The stiffness matrix for the individual plate-strips and beams are then transformed to the chosen global directions after any necessary offset transformations. It is obvious that to evaluate the above stiffnesses, it is necessary to know the loadings on each plate-strip and beam corresponding to any chosen level of total external load on the structure. These individual loadings are dictated by strain compatibility considerations. This is discussed in detail in Ref. 14.

The individual stiffness matrices are appropriately merged resulting in the equation

$$S \cdot D = 0 \tag{34}$$

where S is the merged stiffness matrix of the total structure and is symmetric. D is the vector representing the global displacements of the interlinked junction lines between various plate-strips and beams. As seen earlier, the axial (x) variations of these displacements are the same along all junction lines and have been conveniently dropped from the stiffness equations. Hence the vector D has implied values of $\sin\alpha = 1$ or $\cos\alpha = 1$.

It is obvious that Eq. (34) signifies the equilibrium of the structure in an adjacent deflected (buckled) position. A nontrivial solution exists when the matrix S has a zero determinant, i.e.,

$$|S| = 0 \tag{35}$$

The elements of S are transcendental functions of the external loadings and the axial (x) half-wave length of buckling (a/m).

For a chosen number of half-waves m (or half-wave length) the buckling load is determined from Eq. (35) by an iteration procedure using the algorithm discussed in Ref. 6. A series of m values are investigated and the lowest of all buckling loads is the critical load of the structure. The corresponding vector D is then obtained by the inverse iteration method. The distribution of the buckling displacements across the width of each plate-strip follows from Eq. (24) and (20). The w and v displacements are of prime interest. A plot showing these displacements across the cross section of the structure identifies the weak (buckled) elements and thereby indicates whether buckling is local or general.

The classical buckling analysis usually makes assumptions regarding buckling modes, like Euler mode, torsional mode, local mode, etc. As shown in Ref. 8, such simplifying assumptions could sometimes lead to the possibility of missing the lowest buckling load. The number of buckling half-waves m, in the longitudinal direction must be the same in all elements of the structure. The present analysis makes no assumptions regarding the buckle mode.

The algorithm of Ref. 6 requires an upper bound to the buckling load. This upper bound load is defined as the lowest buckling load of all plate-strips when their interlinked junction lines are completely restrained. This can be readily obtained as shown in Ref. 14 using the Galerkin method.

Some Results

The computer program "BUCLASP2," based on the present analysis is written for the CDC6600 computer. Figure 4 shows the basic layout of the program. Longitudinally stiffened

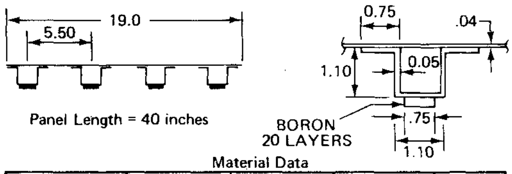

Material Data

Material	$E_{11} \times 10^{-6}$ lbs/in^2	$E_{22} \times 10^{-6}$ lbs/in^2	$G_{12} \times 10^{-6}$ lbs/in^2	ν_{12}
Titanium	16.4	16.4	6.2	0.3
Boron Fiber Composite	29.117	2.341	0.75	0.2467

Results

m	Panel Buckling Load (lbs)		Buckling Strain x 10^3 (in/in)	
	With Offsets	Without Offsets	With Offsets	Without Offsets
1	64520	55770	1.7035	1.4726
2	209800	183100	5.5403	4.8339

Fig. 10 Hat stiffened panel—effect of offsets.

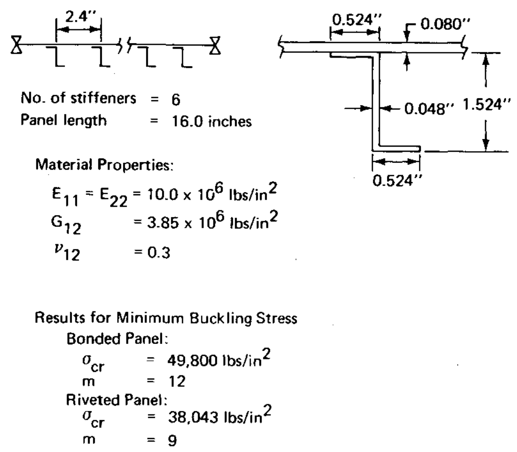

Fig. 11 Zee-stiffened panel—bonded and riveted stiffeners.

structures commonly exhibit repetitiveness of stiffening (e.g., stiffened panels). The computer program contains features which utilize this property to provide operational efficiency, and to simplify the input. A structural panel is modeled as a start substructure, repeat substructure (each repeat substructure has the same stiffness) and an end substructure. The algorithm used in the buckling determinant calculation requires in core the matrices corresponding to the start, end and one repeat substructure. A symmetric gaussian decomposition is performed on the panel stiffness matrix. During the decomposition the number of sign changes (which correspond to the number of roots of the buckling matrix below the trial load) in the determinant is kept track of. The root count is used to decide the value of the new trial load.

Some numerical results from the analysis are now discussed. Figure 5 shows the cross sections of three conceptually recent structural panels, utilizing curved parts. The results of the stability analysis of these panels, subjected to axial compression, are given in Figs. 6 and 7. For panels 1 and 2 the results from the computer program "BOSOR3,"[15] are also shown for comparison. The mode shapes shown indicate the nature of buckling.

Currently there is a dearth of published design data for

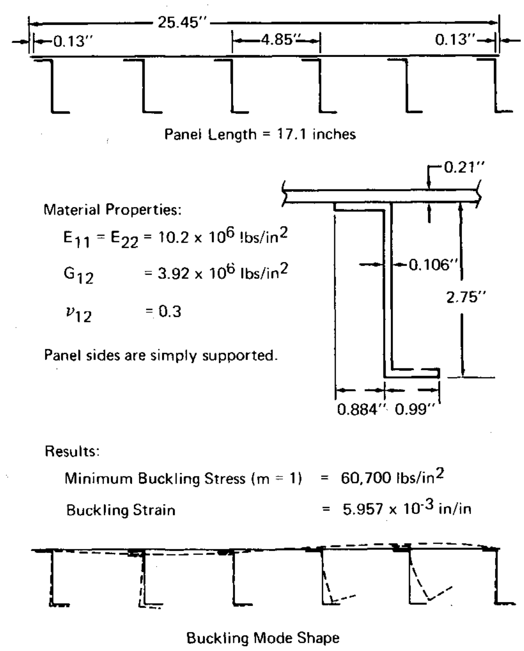

Fig. 12 Zee-stiffened panel—an interesting buckling mode.

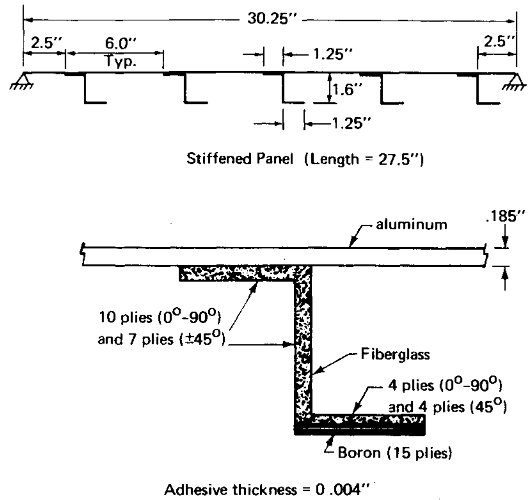

Mat'l	$E_{11} \times 10^{-6}$ (lbs/in^2)	$E_{22} \times 10^{-6}$ (lbs/in^2)	ν_{12}	$G_{12} \times 10^{-6}$ (lbs/in^2)	Ply Thickness (in)
Aluminum	10.5	10.5	.3	4.04	---
Fiberglass (0°-90°)	3.2	3.2	.15	1.0	.01
Fiberglass (±45°)	1.6	1.6	.063	2.0	.01
Boron (0°)	30.0	2.7	.21	0.7	.007

Fig. 13 Composite zee-stiffened panel.

buckling of composite or composite reinforced plates and stiffened plates. "BUCLASP2" may be readily used to generate such data. Figure 8 shows typical interaction curves for a curved plate for two different sets of boundary conditions along the sides. Figure 9 gives two results for a biaxially loaded curved stiffened panel; one where the transverse load is kept constant and the other an interaction curve for the same panel.

The stability analysis presented considers the effect of offsets between various plate-strips and beams. Though sometimes disregarded as in Ref. 16, such offsets can significantly affect the results in certain cases. This is illustrated in Fig. 10 for a composite reinforced hat stiffened panel which is idealized using flat plate-strips only.

Test results of Ref. 17 indicate that riveting stiffeners decrease the skin buckling stress of a zee-stiffened panel by 17% compared to bonding them. By suitable modeling, Ref. 9, the present analysis can differentiate between such connection in an approximate manner. The analysis results in Fig. 11 show the decrease in skin buckling stress to be approximately 22.5%.

Classical stability analyses, because of their implied assumptions regarding the buckling modes (e.g., Euler mode, torsional mode, local mode, etc.), run the risk of missing modes not covered by the assumptions. The results of Fig. 12 show such an example for a zee-stiffened panel. The buckling mode from the present analysis shows a characteristic half-wavelength across the panel width, involving multistiffeners. Prior references to such a mode is not known.

Figure 13 shows a composite stiffened panel. The skin is of aluminum and the outstanding flanges of the glass fiber stiffeners are reinforced with boron fiber composite. The panel buckling loads, strains and mode shapes are shown in Fig. 14. Interesting interactions between various local and over-all deformations are indicated by the mode shapes. These numerical results indicate generality of the stability analysis presented and some of its applications.

References

[1] Giles, G. L., "Structural Efficiencies of Five Compression Panels with Curved Elements," TN D-6479, Dec. 1971, NASA.

[2] Waddoups, M. E., Jackson, S. K., and Rogers, C. W., "The

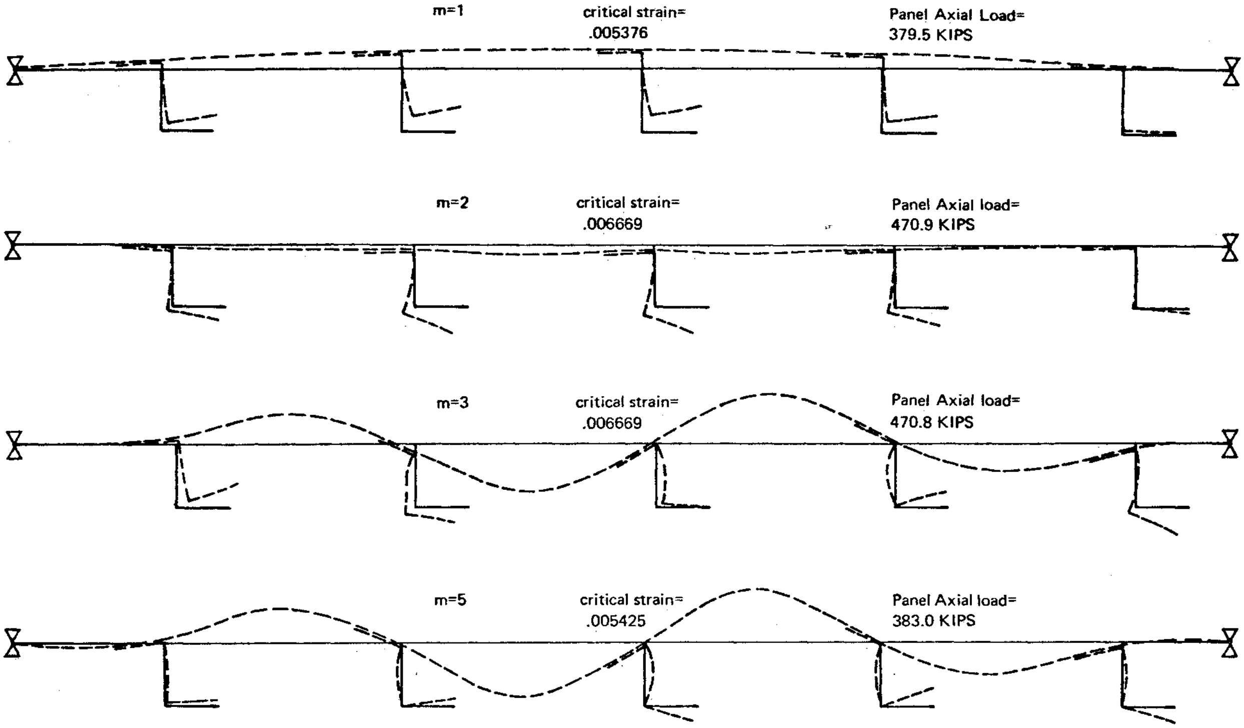

Fig. 14 Buckling modes for the composite zee-stiffened panel.

Integration of Composite Structures into Aircraft Design," *Journal of Composite and Materials,* Vol. 6, April 1972, pp. 174–190.

[3] Viswanathan, A. V., Soong, T.-C., and Miller, R. E., Jr., "Buckling Analysis for Axially Compressed Flat Plates, Structural Sections and Stiffened Plates Reinforced with Laminated Composites," CR-1887, Nov. 1971, NASA.

[4] Williams, F. W., "Bounding of Frame Buckling Loads, Discussion," *Journal of the Structural Division, Proceedings of the American Society of Civil Engineers,* May 1971, pp. 1642–1644.

[5] Novozhilov, V. V., *Thin Shell Theory,* P. Noordhoff, Netherlands, 1964.

[6] Wittrick, W. H. and Williams, F. W., "A General Algorithm for Computing Natural Frequencies of Elastic Structures," *Quarterly Journal of Mechanics and Applied Mathematics,* Vol. 24, Pt. 3, Aug. 1971, pp. 263–284.

[7] Duncan, W. J., "Principles of the Galerkin Method," R & M 1848, Sept. 1938, Aeronautical Research Committee, London, England.

[8] Viswanathan, A. V., Soong, T. C., and Miller, R. E., Jr., "Compressive Buckling Analysis and Design of Stiffened Flat Plates with Multi-layered Composite Reinforcement," *National Symposium on Computerized Structural Analysis and Design,* George Washington Univ., Washington, D.C., March 1972.

[9] Tripp, L. L., Tamekuni, M., and Viswanathan, A. V., "A Computer Program for Instability Analysis of Biaxially Loaded Composite Stiffened Panels and other Structures; User's Manual for BUCLASP2," CR-112226 1973, NASA.

[10] Ashton, J. E., Halpin, J. C., and Petit, P. E., "Primer on Composite Materials: Analysis," *Progress in Material Sciences,* Vol. 3, Technomic Publications, Stamford, Conn., 1969.

[11] Kempner, J., "Unified Thin Shell Theory," Rept. 566, March 1960, Dept. of Aeronautical Engineering and Applied Mechanics, Polytechnic Inst. of Brooklyn, New York.

[12] Novozhilov, V. V., *Foundations of the Nonlinear Theory of Elasticity,* Graylock, Rochester, N.Y., 1953.

[13] Timoshenko, S. P. and Gere, J. M., *Theory of Elastic Stability,* 2nd ed., McGraw-Hill, New York, 1961.

[14] Viswanathan, A. V. and Tamekuni, M., "Elastic Buckling Analysis for Composite Stiffened Panels and other Structures subjected to Biaxial Inplane Loads," CR-2216, 1973, NASA.

[15] Bushnell, D., "Stress, Stability and Vibration of Complex Shells of Revolution: Analysis and Users Manual for 'BOSOR3,' SAMSO TR-69-375, Sept. 1969, Space and Missile System Organization.

[16] Williams, F. W. and Wittrick, W. H., "Numerical Results for the Initial Buckling of Some Stiffened Panels in Compression," *The Aeronautical Quarterly,* Vol. 23, Feb. 1972, pp. 24–40.

[17] Pride, R. A., Royster, D. M., and Gardner, J. E., "Influence of Various Fabrication Methods on Compressive Strength of Titanium Skin Stringer Panels," TN D-5389, Aug. 1969, NASA.